The generalized planar fault energy, ductility, and twinnability of Al and Al–*RE* (*RE* = Sc, Y, Dy, Tb, Nd) at different temperatures: A first-principles study*

Wu Xiao-Zhi(吴小志)[a)b)c)†], Liu Li-Li(刘利利)[c)], Wang Rui(王 锐)[c)], and Liu Qing(刘 庆)[a)b)‡]

[a)] *College of Materials Science and Engineering, Chongqing University, Chongqing* 400044, *China*
[b)] *National Engineering Research Center for Magnesium Alloys, Chongqing University, Chongqing* 400044, *China*
[c)] *College of Physics and Institute for Structure and Function, Chongqing University, Chongqing* 401331, *China*

(Received 22 July 2013; revised manuscript received 4 December 2013; published online 20 April 2014)

The genearlized planar fault energies of Al and Al–*RE* (*RE* = Sc, Y, Dy, Tb, Nd) alloys have been investigated using first-principles methods combined with a quasiharmonic approach. The stacking fault energies, unstable stacking fault energies, and unstable twinning energies decrease slightly with increasing temperature. The ductility parameter *D*, the relative barrier difference δ_{us}^{ut}, and the twinnability τ_a of Al and Al–*RE* alloys at different temperatures have been determined. It is found that the ductilities of Al and Al alloys are nearly the same and the ductilities increase slightly with increasing temperature. The *RE* alloying elements make twinning more likely and the twinnabilities of Al and Al alloys decrease with increasing temperature.

Keywords: twinnability, temperature, generalized planar fault energy

PACS: 61.72.J–, 61.72.Mm, 61.72.Nn **DOI:** 10.1088/1674-1056/23/6/066104

1. Introduction

Deformation twinning (DT) and dislocation motion are two primary and competing deformation mechanisms for plastic deformation in face-centered cubic (fcc) metals and alloys.[1–3] The competition can be quantified by twinnability. Recent molecular dynamics simulations[4,5] as well as mechanistic models[6] show that the generalized planar fault energy (GPFE) curves suggest the preference for twinning in fcc metals and alloys. Tadmor and Hai[7] have shown that the twinning tendency is dependent on the so-called unstable stacking fault energy γ_{us} and unstable twinning energy γ_{ut}, demonstrating the importance of the GPFE curve in revealing the nature of the slip activity.

There are many theoretical studies focused on the qualitative dependence of deformation twinning tendency on the GPFE curve with the first-principles calculations in fcc metals and alloys. For instance, Siegel[8] and Kibey *et al.*[9] have analyzed the twinnabilities in Ni alloys and Cu–Al alloys by means of the GPFE curves, respectively. Similarly, Muzyk *et al.*[10] performed a more systematic calculation of the twinnabilities in Al-base systems, and Al was assumed to be alloyed with Mg, Ca, Zn, Si, and Cu, their results indicated that the most pronounced tendency for mechanical twinning was expected for alloying with Mg. However, all the calculations were limited at 0 K, so theoretical investigations about the effect of temperature on the GPFE curves and twinnabilities of fcc alloys are still very scarce. Saka *et al.*[11] measured the intrinsic temperature-dependent stacking fault energies (SFEs) in Cu–Al alloys by means of *in situ* thermal cycling experiments with a high-voltage electron microscope. Recently, Shang *et al.*[12] performed a systematic study of the temperature-dependent SFEs for dilute Ni-base alloys resulting from induced alias shear deformation by means of the first-principles calculations. To the best of our knowledge, limited studies have focused on the effect of temperature on the GPFE curves for Al, which is the basis of a wide range of alloys.

In this paper, the temperature-dependent GPFE curves of Al and Al–*RE* (*RE* = Sc, Y, Dy, Tb, Nd) alloys are calculated by using the *ab initio* method with the objective of examining the alloying and temperature effects on twinnabilities. Rare-earth (RE) elements are a class of special elements, which are known to be the most effective modifier and recrystallizator for Al alloys.

2. Computational method

2.1. Details of first-principles and phonon calculations

We employ the first-principles total-energy calculations based on the density functional theory (DFT), using the Vi-

*Project supported by the National Natural Science Foundation of China (Grant Nos. 11104361 and 11304403) and the Fundamental Research Funds for the Central Universities, China (Grant No. CQDXWL2012015).

†Corresponding author. E-mail: xiaozhiwu@cqu.edu.cn
‡Corresponding author. E-mail: qingliu@cqu.edu.cn

© 2014 Chinese Physical Society and IOP Publishing Ltd

enna *ab initio* simulation package (VASP),[13,14] to calculate the temperature-dependent GPFE curves of pure Al and Al–*RE* (*RE* = Sc, Y, Dy, Tb, Nd) systems. The effects of the exchange–correlation function are described with the generalized gradient approximation (GGA) of Perdew–Burke–Eruzerhof (PBE).[15,16] The cut-off energy of the plane wave basis set is chosen at 450 eV. The radius of Al is 1.25 Å, and the radii of rare-earth elements Sc, Y, Dy, Tb, and Nd are 1.60 Å, 1.80 Å, 1.75 Å, 1.75 Å, and 1.85 Å, respectively.[17] In order to calculate the GPFE curves of Al and Al alloys accurately at different temperatures, the periodic supercells consisted of 3×3 slab geometries with 12 atomic planes are employed. All these supercells have been arranged into a perfect sequence $\cdots$ABCABCABCABC$\cdots$. For the alloy systems, one Al atom is substituted by a single solute atom within the sixth layer. As shown in Fig. 1, the GPFE curves for the $(111)/[112]$ system are calculated by displacing parts of the model along the [112] direction in two operations. In the first step, the layers numbered 1–6 are displaced over a distance $|\boldsymbol{b}_{\rm p}| = a_0/\sqrt{6}$ along the [112] direction and the stacking fault $\cdots$ABCABCBCABCA$\cdots$ is created. In the second step, the layers numbered 1–5 are displaced in a similar fashion and the deformation twin $\cdots$ABCABCBABCAB$\cdots$ is generated. We have also calculated the GPFE curves using a 14-layer supercell and found that the variations of the calculated GPFEs are less than 0.5 mJ·m^{-2}, in other words, the results of the 12-layer and the l4-layer supercells are reasonably close. A $\sim$ 15-Å vacuum buffer is added in the direction normal to the slip plane to avoid interactions between faults in two neighboring slabs in our test. For these cells, the Brillouin zone integrations are performed using k-point grids $21 \times 21 \times 2$ of the γ- centered Monkhorst–Pack grids.[18] The total energy is converged numerically to less than 1×10^{-6} eV/atom with respect to electronic self-consistency, while the Hellman–Feynman force components acting on the atoms are relaxed to less than 1×10^{-6} eV·Å^{-1}. All the atomic positions in the supercells have been relaxed in the direction perpendicular to the (111) slip plane in order to minimize the forces and the stresses.

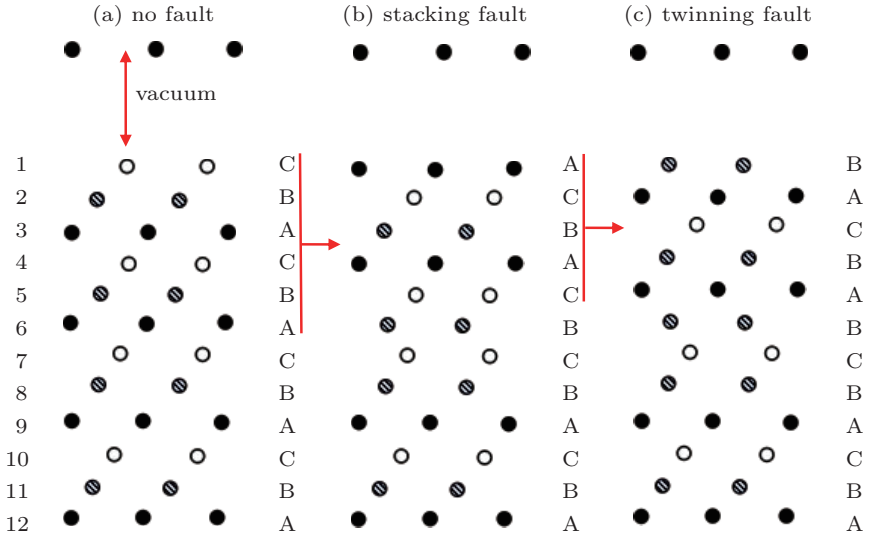


Fig. 1. (color online) A schematic representation of the geometry used to explain the operations leading to the formation of the stacking fault and twin: (a) perfect structure, (b) intrinsic stacking fault structure imposed by sliding layers numbered 1–6 in the upper part, (c) two-layer twin structure imposed by displacing layers 1–5 in a similar fashion. All configurations are separated from the rest by a vacuum. The periodic supercell used here consists of a (2×2) slab geometry with 12 (111) planes.

Phonon calculations are performed for Al by using the supercell approach[19] with the force constants calculated by the VASP interface[14] in the framework of the density-functional perturbation theory[20] and the phonon properties calculated by the PHONOPY package.[21] Here, a $5 \times 5 \times 5$ supercell with 125 atoms is employed based on our test. The forces acting on the atoms for the perturbed supercell are calculated by VASP with a $7 \times 7 \times 7$ Monkhorst k mesh for Al. The other settings of the VASP calculations are the same as those described above. For more details of phonon calculations using the VASP and PHONOPY codes, see, Refs. [21]–[23]. Figure 2 illustrates the calculated phonon dispersions for Al along high-symmetry directions in the Brillouin zone with the theoretical static equilibrium volume at 0 K by the present approach together with the inelastic neutron scattering measurement results.[24,25] It demonstrates that the calculated phonon dispersions of Al accurately reproduce the experiment results.[24,25]

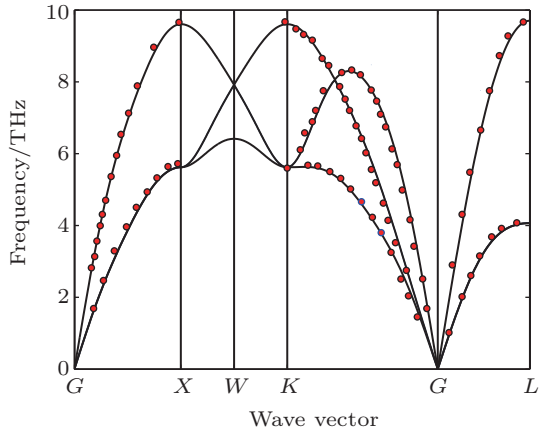


Fig. 2. (color online) Phonon dispersion relations for Al along high-symmetry directions in the Brillouin zone. The circles are from inelastic neutron scattering data.[24,25]

2.2. Thermal expansion

In order to calculate the temperature-dependent GPFE curves for pure Al and Al alloys, we need the lattice constant versus temperature relation $a(T)$. In other words, we need to predict the unit cell volume change as a function of temperature, $V(T)$, which can be determinable from Helmholtz free energy F according to the quasiharmonic approach[26]

$$F(V,T) = E_0(V) + F_{\rm el}(V,T) + F_{\rm mvib}(V,T), \qquad (1)$$

where $E_0(V)$ is the 0-K static total energy, $F_{\rm el}(V,T)$ is the thermal electronic contribution to the Helmholtz energy evaluated from the first-principles calculations directly by assuming that the eigenvalues for the given lattice and nuclear positions are temperature-independent and only the occupation numbers depend on the temperature following the Fermi–Dirac distribution.[27,28] This term is in particular important for metals with non-zero electronic density at the Fermi level. The vibrational contribution to the Helmholtz energy $F_{\rm vib}(V,T)$ is usually described by the phonon approach,[29,30] the empirical Debye model,[30] or the semi-empirical transferable force constant model.[31] In the present work, $F_{\rm vib}(V,T)$ for Al is depicted by a phonon calculation. Here $F(V,T)$ is the free energy per unit cell, and V is the volume per unit cell.

In general, the vibrational free energy $F_{\rm vib}(V,T)$ has both quasiharmonic and anharmonic components. The anharmonic effects which include the phonons interaction and the electron–phonon coupling are weak and can be neglected.[32] Here we work entirely within the quasiharmonic approximation. The familiar result for the remaining quasiharmonic phonon free energy can be written as

$$F_{\rm vib}(V,T) = \sum_k \left[\frac{1}{2}\hbar\omega_k + k_{\rm B}T\ln(1 - {\rm e}^{-\hbar\omega_k/k_{\rm B}T})\right], \qquad (2)$$

where $k_{\rm B}$ represents the Boltzmann constant, $\hbar$ is the reduced Planck constant, and ω_k represents an individual phonon frequency. The summation is over all three phonon branches and over all wave vectors in the first Brillouin zone. It should be noted that in general, phonon frequency ω_k is dependent on the volume, but not on the temperature. The phonon frequency is obtained from the forces resulting from the displacements of certain atoms in the supercell containing $5 \times 5 \times 5$ unit cells, calculated by the VASP code. The vibrational free energy $F_{\rm vib}(V,T)$ is depicted from the phonon calculation performed using the PHONOPY, which can support the VASP code to calculate the force constants directly in the framework of the density-functional perturbation theory.

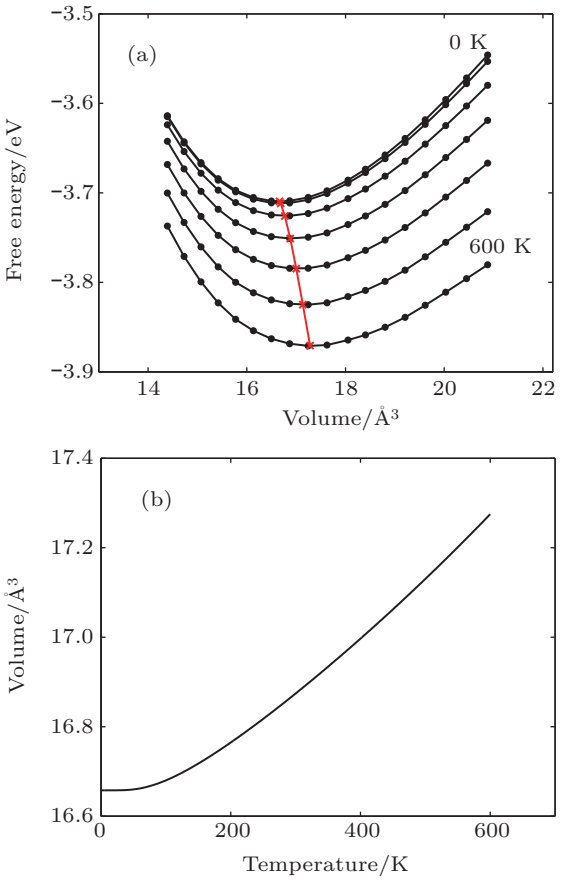


Fig. 3. (color online) (a) Plot of the Helmholtz free energy versus unit cell volume of Al at every 100 K between 0 K and 600 K. The values depicted by the crosses are the equilibrium volumes at corresponding temperature. (b) The equilibrium volume as a function of temperature for Al.

Based on Eq. (1), the estimation of the equilibrium volume V at temperature T is straightforward. We have evaluated the three terms on the right-hand side of Eq. (1) at 18 volume points near the equilibrium volume at 0 K for Al. The volume versus temperature relation $V(T)$ is determined by fitting the Helmholtz free energy F versus volume V (F–V) data according to the Vinet equation of state (EOS).[33] Figure 3(a) illustrates the predicted F as a function of V between 0 K and 600 K at every 100 K for Al, and the value depicted by the red cross at every fitted curve is the equilibrium volume at the corresponding temperature. Obviously, the equilibrium volume increases with increasing temperature (see Fig. 3(b)). Here,

the five Al-based alloys have the same equilibrium volumes at different temperatures with Al due to ∼ 11 at.% RE atoms in one (111) plane and ∼ 0.92 at.% in the supercell.

3. Results and discussion

The calculated temperature-dependent GPFE curves for pure Al and Al alloys by using the supercell consisted of a 3×3 slab geometry with 12 atomic planes are shown in Fig. 4. The first half of each GPFE curve is evaluated by sliding the upper 1–6 atomic layers along the [112] direction over a distance $|\boldsymbol{b}_p| = a_0/\sqrt{6}$.[34,35] The second half is then evaluated in a similar fashion by successively displacing only layers numbered 1–5. The first and the second maxima of each GPFE curve are unstable stacking fault energy (γ_{us}) and unstable twinning energy (γ_{ut}), respectively.[36] The γ_{us} and γ_{ut} represent the minimum energy barriers for partial dislocation[37] and micro-twin nucleation,[38,39] respectively, which are difficult to be obtained from experimental measurements and can only be calculated in the atomistic simulation. The minimum of each GPFE curve is the stable stacking fault energy (γ_{sf}), which can be measured experimentally.

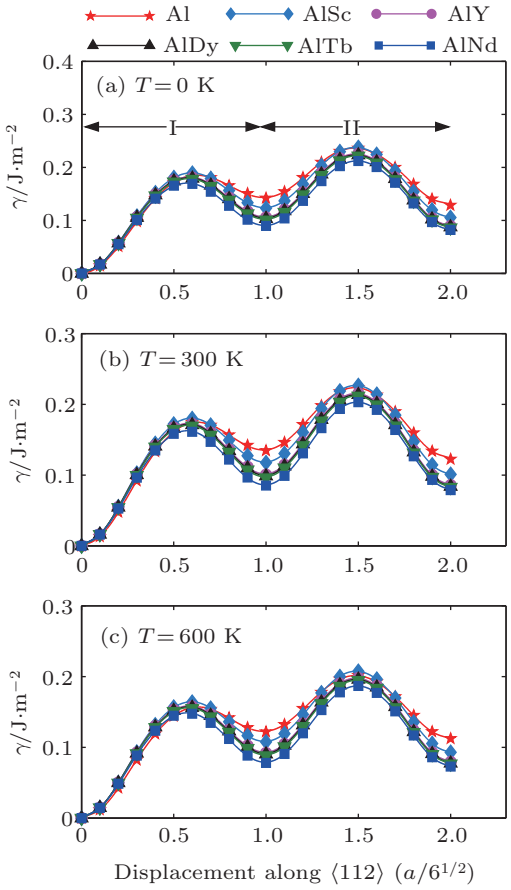


Fig. 4. (color online) The calculated generalized planar fault energy curves for Al and Al alloys at different temperatures. The discrete points denote the values of DFT calculations and the solid curves indicate the results obtained from polynomial fitting.

All the temperature-dependent typical energies (γ_{sf}, γ_{us}, γ_{ut}) for Al and Al alloys calculated using different supercell sizes are listed in Table 1. It is clear that the present typical energies ($\gamma_{sf} = 142$ mJ·m^{-2}, $\gamma_{us} = 185$ mJ·m^{-2}, $\gamma_{ut} = 236$ mJ·m^{-2}) at 0 K for Al nearly agree with the previous DFT calculations ($\gamma_{sf} = 162$ mJ·m^{-2}, $\gamma_{us} = 189$ mJ·m^{-2}, $\gamma_{ut} = 238$ mJ·m^{-2})[10] and the available experimental data ($\gamma_{sf} = 135$ mJ·m^{-2}).[40] It should be noted that the present value of γ_{sf} at 0 K for Al has a larger difference relative to the previous DFT calculation. It may be a result of the fact that our values of the typical energies (γ_{sf}, γ_{us}, γ_{ut}) for Al were obtained with the effect of the zero-point vibrational energy. The typical energies (γ_{sf}, γ_{us}, γ_{ut}) decrease slightly with increasing temperature in the same material, since the thermal expansion may soften the stacking fault configuration at high temperature. Note that the decrease of the stacking fault energy (γ_{sf}) of fcc Ni with increasing temperature has also been predicted.[12]

Table 1. Calculated various fault energies (γ_i, mJ·m^{-2}), ductility parameter (D), relative barrier difference (δ_{us}^{ut}), and theoretical twinnability (τ_a) at different temperatures for Al and Al alloys by using the supercell of a 3×3 slab geometry with 12 atomic planes.

T/K	System	γ_{sf}	γ_{us}	γ_{ut}	D	δ_{us}^{ut}	τ_a
0	Al	142	185	236	1.425	51	0.902
	Al–Sc	123	189	237	1.356	48	0.926
	Al–Y	105	181	225	1.321	44	0.938
	Al–Dy	103	179	223	1.340	44	0.939
	Al–Tb	101	178	222	1.342	44	0.940
	Al–Nd	89	169	212	1.335	43	0.942
300	Al	134	174	223	1.510	49	0.899
	Al–Sc	118	180	227	1.433	47	0.924
	Al–Y	100	172	215	1.399	43	0.937
	Al–Dy	98	171	213	1.419	42	0.938
	Al–Tb	96	169	212	1.421	43	0.939
	Al–Nd	85	161	203	1.417	42	0.941
600	Al	122	156	201	1.647	45	0.896
	Al–Sc	108	164	207	1.588	43	0.921
	Al–Y	92	158	198	1.552	40	0.935
	Al–Dy	90	156	196	1.574	40	0.936
	Al–Tb	88	155	195	1.575	40	0.937
	Al–Nd	78	147	186	1.576	39	0.938

In order to examine how alloying alters the intrinsic ductility of Al at different temperatures, the Rice criterion[37] is employed. Rice has shown that the unstable stacking fault energy γ_{us} is proportional to the energy release rate required for dislocation nucleation, which leads to the ductility parameter $D = 0.3\gamma_s/\gamma_{us}$, where γ_s is the (111) surface energy of pure Al or the selected Al alloys at different temperatures. Dislocation-mediated plasticity occurs when $D > 1$, whereas brittle cleavage fracture occurs when D is small (< 1). The temperature-dependent ductility parameters D for pure Al and selected Al alloys are summarized in Table 1, and displayed in Fig. 5(a) so as to clearly show the ductility parameter change trend with temperature. For pure Al, the calculated $\gamma_s = 877$ mJ·m^{-2} yields $D = 1.42$ at 0 K, indicating that Al

is an intrinsically ductile metal. This is consistent with Mehl's Naval Research Laboratory (NRL) tight-binding (TB) total energy calculations of D for fcc metals,[41] according to which Al ($D = 1.50$) is considerably less ductile than the three noble metals Cu, Ag, and Au ($D > 3$), but substantially more ductile than Rh, Pd, and Ir ($D \approx 1$). Relative to the range of ductility parameters predicted by Rice's criterion, the Al alloys have similar ductilities to the pure Al at different temperatures. The relative insensitivity of D to alloying at this concentration is possibly a result of the fact that these solutes do not alter γ_s of pure Al and γ_{us} in the alloys deviates from pure Al γ_{us} by less than 10%. It should be noted that the Ni alloys have similar variations at 0 K.[8] Besides, the ductilities in the same materials increase slightly with increasing temperature. This may be a result of the fact that the unstable stacking fault energies γ_{us} decrease slightly and the surface energies γ_s are almost unchanged with temperature.

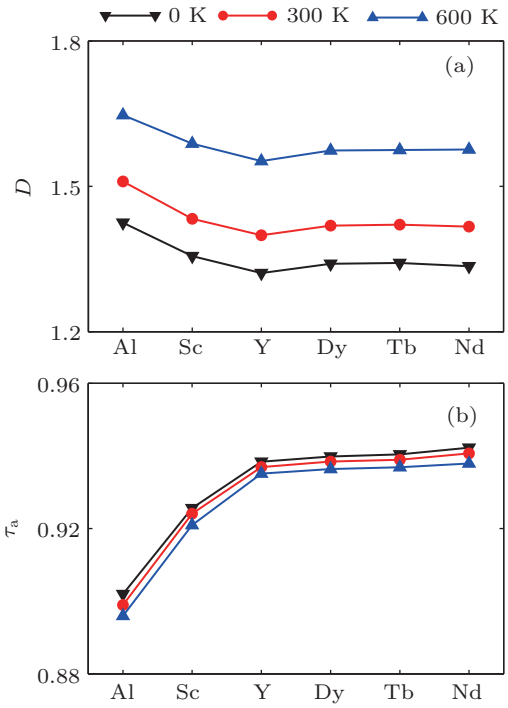


Fig. 5. (color online) The predicted ductility parameters (D) and theoretical twinnabilities (τ_a) for Al and Al alloys at different temperatures. The triangle-down, circle, and triangle-up curves denote the values at 0 K, 300 K, and 600 K, respectively.

In addition to its effects on ductility, we have also investigated whether alloying can alter the mode of plastic deformation at different temperatures. Van Swygenhoven *et al.*[4] proposed that the relative values of γ_{us} and γ_{ut} can describe the ease with which an fcc metal and its alloys deform by twinning relative to deforming by dislocation-mediated slip. According to the analysis, a simple criterion for twinning activation is given by the difference $\delta_{us}^{ut} \equiv \gamma_{ut} - \gamma_{us}$.[37] The temperature-dependent δ_{us}^{ut} for Al and its alloys are listed in Table 1. Obviously, δ_{us}^{ut} decreases significantly with the addition of RE elements, which is primarily due to the lowering of γ_{ut}. This indicates that alloying will make twinning more likely at different temperatures. Furthermore, δ_{us}^{ut} of the same material decreases with increasing temperature, which indicates that the twinnabilities of Al and Al alloys increase with increasing temperature. However, since γ_{ut} is greater than γ_{us} for Al and its alloys at different temperatures, the relative barrier difference δ_{us}^{ut} does not predict twinning to be the dominant deformation mechanism.[9]

A more thorough treatment of the competition between slip and twinning called twinnability has been proposed by Tadmor and Bernstein[38,39] in the form of the following approximate expression:[38,39]

$$\tau_a = \left[1.136 - 0.151\frac{\gamma_{sf}}{\gamma_{us}}\right]\sqrt{\frac{\gamma_{us}}{\gamma_{ut}}}, \tag{3}$$

which clarifies the dependence of twinnability on the material parameters. Here, τ_a is a relative measure of the tendency of a polycrystalline fcc metal to undergo deformation twinning, with higher τ_a indicating a greater propensity for twinning. The computed values of the temperature-dependent τ_a of pure Al and its alloys are listed in Table 1. Our results show that the RE element incorporation can enhance the twinnability of pure Al at different temperatures, which is consistent with the observations of more active twinning systems with more twin-based textures in the alloys.[42,43] This is very similar to the previous investigations of Ni[8] and Cu[9] at 0 K. Thus, the twinnability measure predicts correct trends for twinning in Al alloys at different temperatures. Al alloys have greater twinnabilities than Al both because they have significantly smaller γ_{sf} and because their γ_{ut} are seriously decreased relative to their γ_{us} (see Table 1). In order to see clearly the dependence of the twinnability on the temperature, figure 5(b) presents a plot of τ_a versus the RE elements at different temperatures. It is clear from the figure that the twinnabilities of Al and Al alloys predicted by τ_a decrease with increasing temperature. It is well known that the deformation twinning becomes more favorable over slip at low temperatures and/or high strain rates.[39] Obviously, the results predicted by δ_{us}^{ut} and τ_a have some differences. However, the twinnability criterion τ_a clarifies the deformation twinning dependence on γ_{ut} and γ_{us} in addition to γ_{sf}. The twinning criterion δ_{us}^{ut} based on the relative barrier difference can roughly reflect the mode of plastic deformations of fcc metals and alloys. In other words, the twinnability criterion τ_a can predict the deformation twinning in Al and its alloys more accurately than δ_{us}^{ut}.

4. Conclusion

In summary, the GPFE curves as a function of temperature for pure Al and Al–*RE* (*RE* = Sc, Y, Dy, Tb, Nd) alloys have been investigated by using a supercell of a 3×3 slab

geometry with 12 atomic planes from first-principles calculations. The ductility parameter D, the relative barrier difference δ_{us}^{ut}, and the twinnability τ_a for Al and Al alloys at different temperatures have been determined with the aid of the typical energies. It is found that the ductilities of the alloys are similar to that of Al and the ductilities in the same materials increase slightly with increasing temperature. Our results show that alloying will make twinning more likely. This mechanical behavior is primarily due to a decrease in stacking fault energies γ_{sf} and a relatively larger decrease in unstable twinning energies γ_{ut} which dominates a smaller decrease in the unstable stacking energies γ_{us}. Furthermore, the twinnabilities of Al and Al alloys decrease with increasing temperature.

References

[1] Hirth J P and Lothe J 1982 *Theory of Dislocations*, 2nd edn. (New York: John Wiley)
[2] Christian J W and Mahajan S 1995 *Prog. Mater. Sci.* **39** 1
[3] Xie H X, Wang C Y, Yu T and Du J P 2009 *Chin. Phys. B* **18** 251
[4] Swygenhoven H V, Derlet P M and Froseth A G 2004 *Nat. Mater.* **3** 399
[5] Frøseth A G, Derlet P M and Swygenhoven H V 2004 *Appl. Phys. Lett.* **85** 5863
[6] Asaro R J and Suresh S 2005 *Acta Mater.* **53** 3369
[7] Hai S and Tadmor E B 2003 *Acta Mater.* **51** 117
[8] Siegel D J 2005 *Appl. Phys. Lett.* **87** 121901
[9] Kibey S, Liu J B, Johnson D D and Sehitoglu H 2006 *Appl. Phys. Lett.* **89** 191911
[10] Muzyk M, Pakiela Z and Kurzydlowski K J 2011 *Scr. Mater.* **64** 916
[11] Saka H, Sueki Y and Imura T 1978 *Philos. Mag. A* **37** 273
[12] Shang S L, Wang W Y, Wang Y, Du Y, Zhang J X, Patel A D and Liu Z K 2012 *J. Phys.: Condens. Matter* **24** 155402
[13] Kresse G and Hafner J 1993 *Phys. Rev. B* **47** 558
[14] Kresse G and Furthmuller J 1996 *Phys. Rev. B* **54** 11169
[15] Perdew J P, Burke K and Ernzerhof M 1996 *Phys. Rev. Lett.* **77** 3865
[16] Perdew J P, Burke K and Ernzerhof M 1996 *Phys. Rev. Lett.* **78** 1396
[17] Slater J C 1964 *J. Chem. Phys.* **41** 3199
[18] Monkhorst H J and Pack J D 1976 *Phys. Rev. B* **13** 5188
[19] van de Walle A and Geder G 2002 *Rev. Mod. Phys.* **74** 11
[20] Kresse G, Marsman M and Furthmüller J *VASP the Guide* http://cms.mpi.univie.ac.at/vasp/
[21] Togo A, Oba F and Tanaka I 2008 *Phys. Rev. B* **78** 134106
[22] Togo A, Chaput L, Tanaka I and Hug G 2010 *Phys. Rev. B* **81** 174301
[23] Togo A 2009 *Phonopy* http://phonopy.sourceforge.net/
[24] de Gironcoli S 1995 *Phys. Rev. B* **51** 6773
[25] Savrasov S Y and Savrasov D Y 1996 *Phys. Rev. B* **16** 487
[26] Moriarty J A, Belak J F, Rudd R E, Sŏerlind P, Streitz F H and Yang L H 2002 *J. Phys.: Condens. Matter* **14** 2825
[27] Wasserman E, Stixrude L and Cohen R E 1996 *Phys. Rev. B* **53** 8296
[28] Sha X W and Cohen R E 2010 *Phys. Rev. B* **81** 095105
[29] Wang Y, Liu Z K and Chen L Q 2004 *Acta Mater.* **52** 2665
[30] Shang S L, Wang Y, Kim D E and Liu Z K 2010 *Comput. Mater. Sci.* **47** 1040
[31] Liu J Z, Ghosh G, van de Walle A and Asta M 2007 *Phys. Rev. B* **75** 104117
[32] Orlikowski D, Söderlind P and Moriarty J A 2006 *Phys. Rev. B* **74** 054109
[33] Vinet P, Rose J H, Ferrante J and Smith J R 1989 *J. Phys.: Condens. Matter* **1** 1941
[34] An M R, Song H Y and Su J F 2012 *Chin. Phys. B* **21** 106202
[35] Shao Y F, Yang X, Zhao X and Wang S Q 2012 *Chin. Phys. B* **21** 093104
[36] Wu X Z, Wang S F and Liu R P 2009 *Chin. Phys. B* **18** 2905
[37] Rice J R 1992 *J. Mech. Phys. Solids* **40** 239
[38] Bernstein N and Tadmor E B 2004 *Phys. Rev. B* **69** 094116.
[39] Tadmor E B and Bernstein N 2004 *J. Mech. Phys. Solids* **52** 2507
[40] Smallman R E and Dobson P S 1970 *Metall. Trans.* **1** 2383
[41] Mehl M J, Papaconstantopoulos D A, Kioussis N and Herbranson M 2000 *Phys. Rev. B* **61** 4894
[42] Basinski Z S, Szcerba M S and Embury J D 1997 *Philos. Mag. A* **76** 743
[43] Ratuszek W and Karp J 1976 *Met. Sci.* **10** 214